Microstructure evolution of highly ordered $Bi_4Si_3O_{12}$ microcrystals

Qingquan Tian[1,*], Xiufeng Wang[2]

[1]*School of Chemistry and Materials, Weinan Normal University, Weinan, 714099, Peoples R China*

[2]*School of Materials Science and Engineering, Shaanxi University of Science & Technology, Xi'an, 710021, Peoples R. China*

Received 25 January 2026; received in revised form 27 March 2026; accepted 30 March 2026

Abstract

This study reports the preparation of dendritic bismuth silicon oxide ($Bi_4Si_3O_{12}$) microcrystals by using solid state reaction stages and heating of Bi_2O_3-SiO_2 powder mixture at 800 °C for different holding times and ambient conditions. X-ray diffractometer (XRD) and scanning electron microscopy (SEM) were used to analyse the prepared microcrystals. XRD analysis revealed that microcrystals showed the eulytite structure, with a gradual decrease in the proportion of $Bi_{12}SiO_{20}$ phase and a considerable increase in $Bi_4Si_3O_{12}$ phase as the holding time increased during heating at 800 °C. This phenomenon is attributed to the occurrence of a transformation in the system, change of crystal composition and generation of dendritic-structured microcrystals by increasing the holding time. An ordered structure similar to typical preferential orientation growth was formed with the growing epitaxial structure of $Bi_4Si_3O_{12}$ grains on the favourable microcrystal surface. However, the domain structure gradually disappeared after a certain period.

***Keywords**: bismuth silicon oxides, microstructure evolution, highly ordered structure, eulytite structure*

I. Introduction

Crystalline bismuth silicon oxides ($Bi_{12}SiO_{20}$, Bi_2SiO_5 and $Bi_4Si_3O_{12}$) have attracted greater scientific significant interest due to their excellent properties [1–3]. As a crucial scintillator and photorefractive material [4,5], $Bi_{12}SiO_{20}$ is widely used in electro optics, acoustics and piezotechnics, whereas $Bi_4Si_3O_{12}$ demonstrates outstanding optical and electrical properties [1,6,7]. Due to their fast response and cost-effectiveness [8], an eulytite-structured $Bi_4Si_3O_{12}$ crystal is a promising alternative to bismuth germanium oxide ($Bi_4Ge_3O_{12}$) in certain cases. The growth of $Bi_4Si_3O_{12}$ crystals has so far been investigated using the Bridgman method [4,9]. In addition to the accuracy of elastic and dielectric constants, the defects and relative stability of $Bi_{12}SiO_{20}$ and $Bi_4Si_3O_{12}$ are also demonstrated to have great significance [2,10]. However, a comprehensive analysis of the phase relation and the crystallographic properties of the system remains limited due to the complexity of the Bi_2O_3-SiO_2 binary melt [11]. Previous studies demonstrated significant differences between metastable states compared to the unique stable equilibrium state [6, 11]. Melt cooling considerably influenced the structure of metastable materials in the Bi_2O_3-SiO_2 binary system at various experimental conditions, including melt components and melting temperatures [12]. The relationship between the heat treatment method and the product composition of the Bi_2O_3-SiO_2 binary melt was examined theoretically and experimentally [2,12,13]. The state of developing crystalline phases is extensively influenced by the initial cooling temperature. Bermeshev *et al*. [14,15] stated the impact of melt cooling conditions on the phase composition of these crystalline phases. Furthermore, the surface condition and microstructure of the melt are essential to all melt components and melting temperatures-related applications, which are examined with melt cooling and solidification conditions [16,17]. Previous studies reported the relationship between melt cooling conditions and the morphology of developing crystals [18–20].

Phase separation in the Bi_2O_3-SiO_2 binary melt takes place at high temperatures. The characteristics and impact of the metastable melt that developed following binary mixture melting are unclear according to the phase equilibrium. In a previous study, sintering was used to form highly ordered $Bi_4Si_3O_{12}$ microcrystals at ambient conditions [21], and to examine the link between highly organized grain-like structure and the distribution of grain sizes

*Corresponding author: tel: +86 913 2136930
e-mail: *qqtian12b@alum.imr.ac.cn*

in $Bi_4Si_3O_{12}$ microcrystals [21,22]. However, there are few and insufficient investigations on various thermal treatment techniques to examine the morphology of the crystalline phases in the Bi_2O_3-SiO_2 binary system. This study verified the influence of time on the microstructure of highly ordered $Bi_4Si_3O_{12}$ grains and explored their crystalline morphology. The effect of heat treatment on the phase composition and microstructure of the prepared crystalline phases of a melt with 50 mol% Bi_2O_3 and 50 mol% SiO_2 was studied. The effect of time on the growth of highly ordered $Bi_4Si_3O_{12}$ microcrystals was investigated at 800 °C under ambient conditions.

II. Experimental

Bi_2O_3 and SiO_2 powders (99.99% purity) were mixed on 1:1 mole ratio, thoroughly milled with an agate mortar and homogenized with a pestle in ethanol at room temperature for 3 h. After the infrared drying, the obtained Bi_2O_3-SiO_2 were evenly classified into six samples. The samples were placed in a corundum crucible in the air and covered with a lid, followed by calcination in a box furnace at 800 °C for 0.5, 1, 2, 4, 6 and 10 h at a heating rate of 10 °C/min. After cooling to room temperature, the samples were removed from the cooled furnace hearth, and the resulting samples were designated as BSO-*x* where *x* = 0.5, 1, 2, 4, 6 and 10, respectively.

A powder X-ray diffractometer (XRD, Rigaku, Japan, D/max 6100PC) was used to analyse the crystalline phases of the heat-treated samples. The effect of holding time on the microstructure at high temperatures was evaluated using Cukα irradiation at 30 kV and 15 mA, with 2θ ranging from 10° to 70° at a scanning rate of 0.02 °/s. The surface morphological analysis of samples was investigated using scanning electron microscopy (SEM, Sigma500, Zeiss, Germany).

III. Results and discussion

XRD patterns of the BSO-*x* samples heat-treated at 800 °C for 0.5, 1, 2, 4 and 6 h are presented in Fig. 1. All samples exhibited very intense diffraction peaks, indicating highly crystalline phases, which are consistent with the standard data of cubic $Bi_4Si_3O_{12}$ eulytite and $Bi_{12}SiO_{20}$ sillenite structures. Compared to the JCPDS cards, several diffraction peaks indicated considerable changes in the relative intensity, which can be attributed to the growth of crystals according to their preferred orientation during heating.

XRD patterns of the BSO-0.5 sample (Fig.1) indicates presence of crystalline $Bi_4Si_3O_{12}$ and $Bi_{12}SiO_{20}$ phases with a significant proportion of unreacted Bi_2O_3 and SiO_2, representing insufficient time for the completion of solid reaction. XRD pattern of the BSO-1 sample (Fig. 1) shows a significant increase in crystallinity with increasing annealing time to 1 h, which suggested the formation of $Bi_{12}SiO_{20}$ and $Bi_4Si_3O_{12}$ phases as the main products with a small amount of the Bi_2O_3 and SiO_2. Moreover, a significant increase in the intensity of the diffraction peak of the $Bi_{12}SiO_{20}$ and $Bi_4Si_3O_{12}$ phases was observed. However, the diffraction peaks of $Bi_{12}SiO_{20}$ phase are stronger, displaying the preferential formation of this phase during the reaction at a high temperature. In the BSO-2 sample, the diffraction peak intensity of $Bi_4Si_3O_{12}$ phase increases while that of $Bi_{12}SiO_{20}$ phase decreases, indicating an increase and decrease in the $Bi_4Si_3O_{12}$ and $Bi_{12}SiO_{20}$ contents, respectively. Furthermore, the BSO-4 and BSO-6 samples show weak diffraction peaks of $Bi_{12}SiO_{20}$ phase, while those corresponding to $Bi_4Si_3O_{12}$ phase are sharp and strong, thus suggesting the oriented growth of $Bi_4Si_3O_{12}$ grains with increasing heating time.

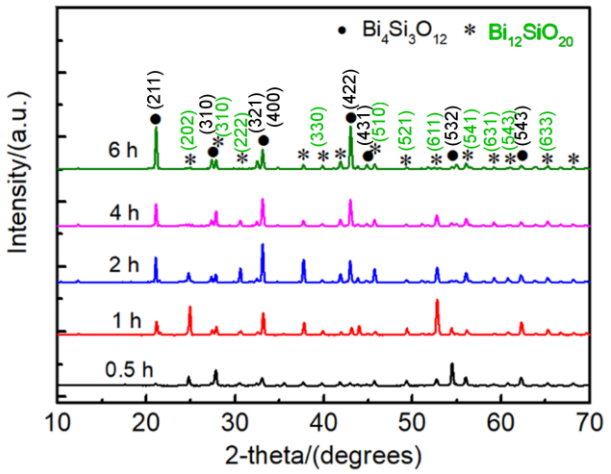

Figure 1. XRD patterns of the heated Bi_2O_3-SiO_2 samples at different holding times (i.e. 0.5, 1, 2, 4 and 6 h)

The increased proportion of $Bi_4Si_3O_{12}$ phase considerably decreased the proportion of $Bi_{12}SiO_{20}$ phase, which can be attributed to its dissolution or transformation into other compounds. $Bi_{12}SiO_{20}$ did not completely disappear, but rather declined in comparison to the formation of $Bi_4Si_3O_{12}$ phase. The gradual increase and decrease of the phases proposed an active process in which a phase changed or evolved into another under specific conditions.

SEM was also used to analyse the growth mechanism of the crystals in the Bi_2O_3-SiO_2 binary system. As illustrated in Fig. 2, the SEM image of the BSO-0.5 sample heated at 800 °C demonstrated the formation of fine equiaxed grains with a characteristic solid-liquid interface mainly due to the rapid cooling over the short period and the lack of thermal equilibrium at the furnace wall. A few quadrangle grains observed in the BSO-0.5 sample made contact with the unreacted melt to prevent interspace formation. $Bi_{12}SiO_{20}$ was formed as the major phase in the previous study of heating analysis

of Bi_2O_3-SiO_2 [6]. The solid state reaction was used to form the $Bi_4Si_3O_{12}$ phase as the product with increasing temperature to 743 °C. Due to the absence of voids between the grains, the product showed the presence of a few non-reactive melts as residues, suggesting the suitability of a short time to form $Bi_{12}SiO_{20}$.

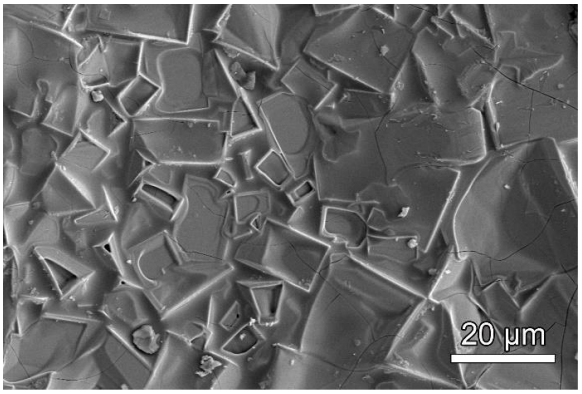

Figure 2. SEM image of the Bi_2O_3-SiO_2 heated at 800 °C at a holding time of 0.5 h

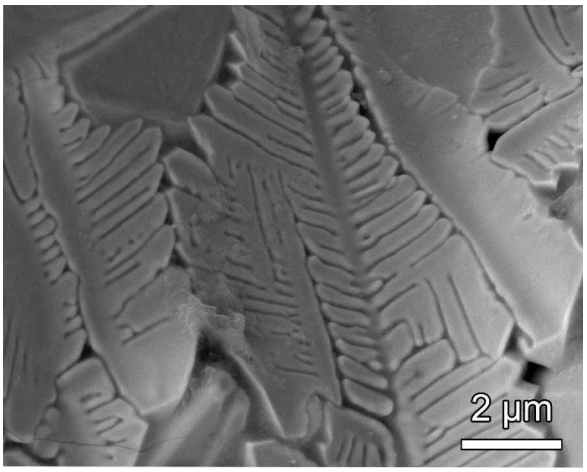

Figure 3. SEM image of the Bi_2O_3-SiO_2 heated at 800 ℃ at a holding time of 1 h

SEM image of the BSO-1 sample at 800 ℃ for 1 h (Fig. 3) suggested a highly ordered, seaweed like growth that is growing outward from the primary arms at an angle of ~90°. The growing structure splits after bending away from the primary arm to form seaweed-like microcrystals. Dendritic crystals with several branches were formed, followed by the development of a large number of secondary dendrites on the primary branch. The primary dendritic arms were short. The dendrites progressively diminished as the branch grains of the dendrite became smaller. The secondary dendritic arms were longer, along with a short distance between the adjacent dendrites, presenting fewer voids on the surface of the BSO-1 sample. $Bi_4Si_3O_{12}$ grains are less developed, but the grains remain close. The secondary dendritic arms grew along the branch upwards due to the limited space, forming incomplete branching patterns with fully developed dendrites like seaweed on their left and right. Each grain in one single line was adjacent to two close-packed grains that formed a periodic structure in a line.

SEM image of the BSO-2 sample heated at 800 ℃ for 2 h is shown in Fig. 4. Compared to the BSO-1 microstructure, the $Bi_4Si_3O_{12}$ crystals of the BSO-2 sample showed highly ordered columnar dendrites growing epitaxially over the adjacent secondary dendrite arms. The dendrite arms displayed an average length and width of 5–20 and ~2–3 µm, respectively, with the growth remaining parallel to one another and parallel to the growth direction of the neighbouring columnar dendrites. However, in the previous layer, the primary dendrites exhibited growth direction perpendicular to that of secondary dendrites. The primary dendrites developed epitaxially from secondary dendrites. The supply of the melt was effectively prevented by the contact of primary and secondary dendrites, thus forming pores and shrinkages.

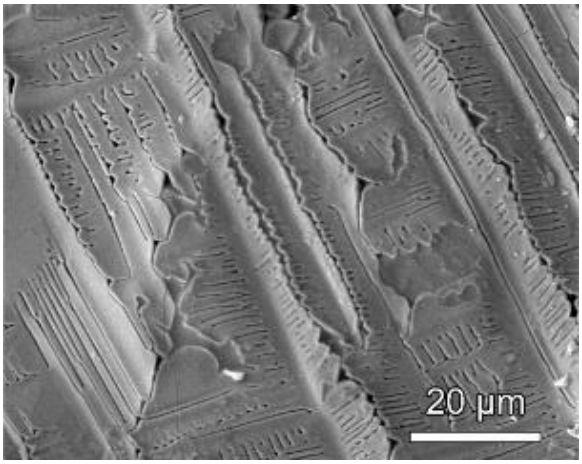

Figure 4. SEM imageimage of Bi_2O_3-SiO_2 heated at 800 ℃ at a holding time of 2 h

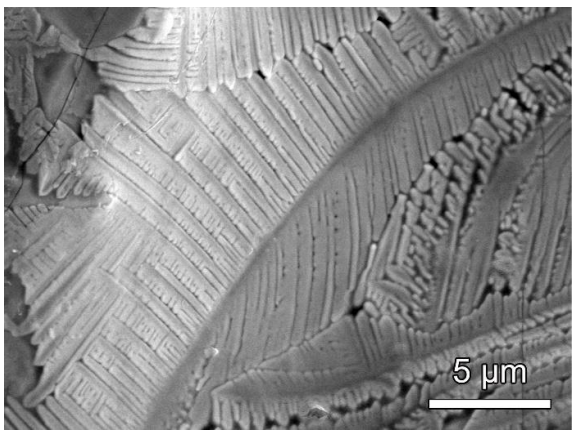

Figure 5. SEM image of Bi_2O_3–SiO_2 heated at 800℃ at a holding time of 4 h

SEM image of the BSO-4 sample heated at 800 ℃ for 4 h displayed the main products of seaweed-like $Bi_4Si_3O_{12}$ crystals with a few $Bi_{12}SiO_{20}$ grains (Fig. 5). Compared to the BSO-1 sample, the primary arms showed the growth of a highly branched structure at an angle <90°. The long and thick secondary dendrites were

oriented perpendicularly to the primary dendrite branch. The well-grown secondary dendrites existed over an extended zone. As the neighbouring dendrites occupied the growing space, the dendrite growth deviated from its original direction due to the lack of space. The growing arms grew in a zig-zag pattern by bending away from the primary arm during the branch growth. The seaweed-like structures may be disturbed throughout the solid-state reaction because of the melt consumption by the adjacent branched grains. The dendrite arms of the BSO-4 sample did not grow at a 90° angle from each other, suggesting a different growth direction compared to the BSO-1 sample.

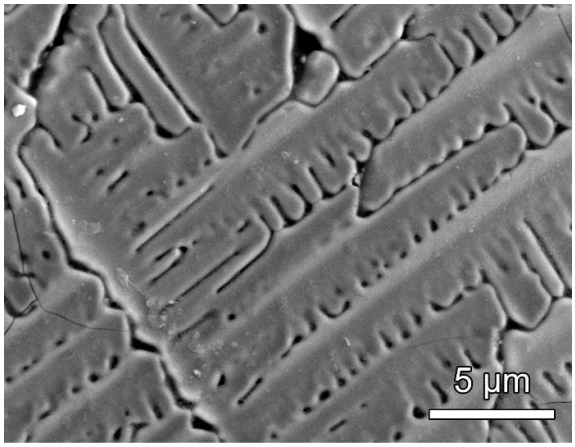

Figure 6. SEM image of Bi_2O_3-SiO_2 heated at 800°C at a holding time of 6 h

SEM image of the BSO-6 sample heated at 800 °C for 6 h comprised dendrites compared to the structure of the BSO-1 and BSO-2 samples, as illustrated in Fig. 6. The highly ordered columnar dendrites grew epitaxially over the neighbouring secondary dendrite arms. The dendrite arms demonstrated an average length and width of 10–20 and ~2–3 µm, respectively. In line with the BSO-2 sample, the growth directions of the adjacent columnar dendrites were parallel to one another, while those of the primary dendrites were perpendicular to the secondary dendrites in the previous layer, indicating the epitaxial growth of primary dendrites from secondary dendrites. Dendrites were produced with the competitive growth and continuously forming dendrites in the solid–liquid phase during sufficiently stable holding time. The melt phase was separated through the interaction of the primary and secondary dendrite arms, resulting from various primary dendrites. The system indicated the existence of the slender dendrite arms due to the complete reaction of the molten solid.

As presented in Fig. 7a, SEM image of the BSO-10 sample heated at 800 °C for 10 h displayed a surface free of dendrites or seaweed-like structures comparable to samples heated for a period of less than 10 h. It has a dense, void-free architecture. Numerous crescent-row stripes were formed on its surface, similar to the cleavage plane of a single crystal at high reaction temperature. The BSO-10 surfaces showed flake-like structures covered by a cleavage plane, obtaining the eulytite structure with large-sized, low nucleation grains, indicating the significant influence of time on the growth orientation and rate at high temperatures.

XRD pattern of the BSO-10 sample exhibited strong intensity of the diffraction peaks of the eulytite structure (JCPDS card No. 35-1007), displaying the high crystallinity of the $Bi_4Si_3O_{12}$ phase in the BSO-10 sample, as presented in Fig. 7b. These diffraction peaks can be correlated with the indices of the lattice plane of the crystalline cubic phase of $Bi_4Si_3O_{12}$, comparable to the findings shown in Fig. 1. The strong diffraction peaks at 27.4° and 56.5°, corresponding to (310) and (620) planes, unlike the conventional data of the eulytite structure, demonstrate the growth of preferential orientation growth of $Bi_4Si_3O_{12}$ phase in the main plane (310).

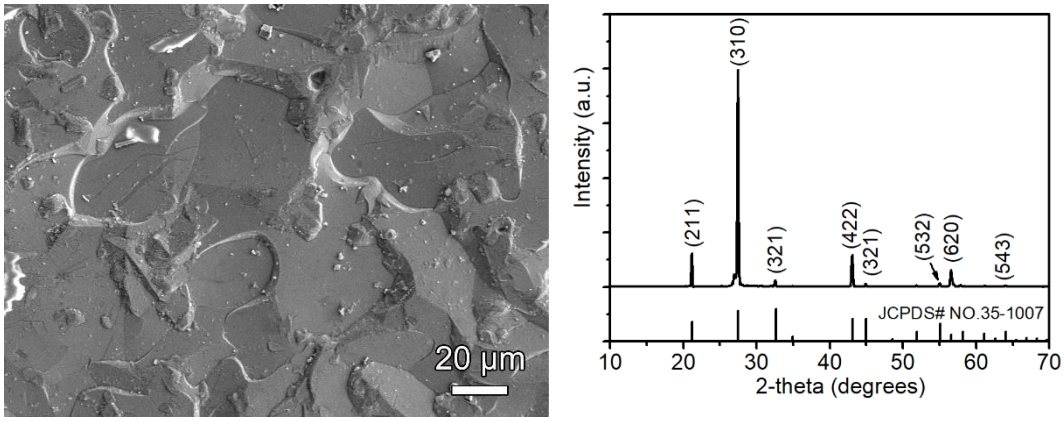

a) b)

Figure 7. SEM image (a) and XRD patterns (b) of Bi_2O_3-SiO_2 heated at 800 °C at a holding time of 10 h

To further enhance the growth of a highly ordered $Bi_4Si_3O_{12}$ structure, several factors must be considered, including the following. The surface and interface areas, along with the strain energy of differently oriented microcrystal grains, must be minimized by regulating the thermodynamic conditions of the phase equilibrium that

determine the driving force for the growth of an ordered structure [23,24]. The microstructure of microcrystals evolved depending on the velocity at the solid liquid interface and the undercooling ΔT before the solidification of individual phases in the Bi_2O_3-SiO_2 system [25]. Undercooled melts constitute a significant driving force for the formation of crystals generated by the difference in the Gibbs free energy of the crystal nucleus and metastable liquid states [26]. The formation of a highly ordered structure is also influenced by the grain spacing. During the growth of a highly ordered structure, melt accumulation started early with closed $Bi_4Si_3O_{12}$ grains, which significantly increased the growth rate and caused the formation of a branched morphology [27]. Given the same conditions under furnace cooling, the closely placed $Bi_4Si_3O_{12}$ grains suggested that melt accumulation could start earlier in the growth process of the highly ordered structure. The close-packed $Bi_4Si_3O_{12}$ grains exhibited a higher probability of melt accumulation earlier during the growth process, which significantly slowed the growth rate and eventually formed branched morphologies [28]. Therefore, preferential orientation growth was formed by the development of the highly ordered, epitaxial structure of eulytite along the favourable microcrystal surface, and their growth can be promoted and controlled by considering the optimization of the governing factors.

V. Conclusions

This study investigated the structure of $Bi_4Si_3O_{12}$ and $Bi_{12}SiO_{20}$ crystals formed by solid-phase reaction under normal pressure in the Bi_2O_3-SiO_2 system at 800 °C for various times. During the solid-state reaction, high amount of $Bi_{12}SiO_{20}$ crystals were successfully formed in the Bi_2O_3-SiO_2 mixture at 800 ℃ and shorter holding times. The $Bi_4Si_3O_{12}$ content in the system was progressively increased as the time increased, while that of $Bi_{12}SiO_{20}$ gradually decreased. A dendrite $Bi_4Si_3O_{12}$ structure was formed first, followed by the gradual disappearance of the domain structure after a certain period. During the heating period, the dendritic structure was produced by the competitive growth and continuous formation of dendrites in the solid-liquid phase. The growth of the epitaxial structure of $Bi_4Si_3O_{12}$ grains along the favourable microcrystal surface results in the formation of a highly ordered structure of typical preferential orientation growth.

Acknowledgement: This work was financially supported by the Scientific Research Program Funded by Weinan Normal University (No. 18ZRRC03). The authors would like to thank all the reviewers who provided constructive comments, as well as MJEditor (www.mjeditor.com) for polishing the English editing services during the manuscript preparation.

References

1. M.V. Lalic, S.O. Souza, "The first-principles study of electronic and optical properties of BGO and BSO scintillators", *Opt Mater.*, **30** (2008) 1189–1192.
2. M.V.d.S. Rezende, C.W.A. Paschoal, M.E.G. Valerio, R.A. Jackson, "Computer modelling of $Bi_{12}SiO_{20}$ and $Bi_4Si_3O_{12}$: Intrinsic defects and rare earth ion incorporation", *J. Solid State Chem*., **292** (2020) 121608.
3. K. Sakamoto, M. Hagiwara, H. Taniguchi, S. Fujihara, "Fabrication of bismuth silicate Bi_2SiO_5 ceramics as a potential high-temperature dielectric material", J. Mater. Sci., **56** (2021) 8415–8426.
4. V.M. Skorikov, Y.F. Kargin, A.V. Egorysheva, V.V. Volkov, M. Gospodinov, "Growth of sillenite-structure single crystals", *Inorg. Mater*., **41** (2005) S24–S46.
5. B. Lal, S.K. Patro, S. Singh, "Nano-sized polycrystalline bismuth silicon oxide powder by sol-gel techniques", *J. Sol-Gel Sci. Technol*., **56** (2010) 340–344.
6. B. Onderka, K. Fitzner, M. Kopyto, B. Przybylo, "Thermodynamics of Bi_2O_3-SiO_2 system", *J. Mining Metal. B Metal.*, **53** (2017) 223–231.
7. T. Maeder, "Review of Bi_2O_3-based glasses for electronics and related applications", *Int. Mater. Rev*., **58** (2013) 3-40.
8. A.F. Lima, S.O. Souza, M.V. Lalic, "Electronic structure and optical absorption of the $Bi_4Ge_3O_{12}$ and the $Bi_4Si_3O_{12}$ scintillators in ultraviolet region: An *ab initio* study", *J. Appl. Phys*., **106** (2009) 013715.
9. Y.T. Fei, S.J. Fan, R.Y. Sun, J.Y. Xu, M. Ishii, *Prog. Cryst. Growth Ch.*, **40** (2000) 189–194.
10. A. Sadeghzadeh-Attar, S. Hajijafari-Bidgoli, M.R. Bafandeh, "Structure and dielectric behaviour of Sr-modified $Bi_4Si_3O_{12}$ thin films prepared via sol gel method", *Process. Appl. Ceram*., **12** [1] (2018) 36–44.
11. V.P. Zhereb, V.M. Skorikov, "Effect of metastable phases on the structural perfection of single crystals of stable bismuth oxide compounds", *Inorg. Mater*., **39** (2003) 1181–1187.
12. T.V. Bermeshev, V.P. Zhereb, R.N. Tas-Ool, E.V. Mazurova, S.I. Metelitsa, Phase separation in the Bi_2O_3-SiO_2 system. Effect of cooling conditions on the phase composition and microstructure of solidification products, *Russ. Chem. B*, **70** (2021) 1462–1470.
13. T.V. Bermeshev, V.P. Zhereb, M.P. Bundin, A.N. Zaloga, A.S. Yasinsky, O.V. Yushkova, D.S. Voroshilov, E.Y. Podshibyakina, I.Y. Gubanov, E.V. Mazurova, A.B. Nabiulin, V.P. Chentsov, V.V. Ryabov, O.V. Yakivyuk, "Modeling of the $Bi_2O_3 \cdot SiO_2$ melt cooling process and the products of melt solidification under various conditions", *Inorg. Mater*., **58** (2022) 1058–1064.
14. T.V. Bermeshev, V.P. Zhereb, M.P. Bundin, A.S. Yasinsky, O.V. Yushkova, D.S. Voroshilov, A.S. Samoilo, E.V. Mazurova, A.N. Zaloga, O.V. Yakivyuk, V.M. Bespalov, "Effect of heat treatment of molten Bi_2O_3 containing 22 mol% SiO_2 on the state of the metastable δ*-phase forming during solidification", *Inorg. Mater*., **58** (2022) 604–611.
15. T.V. Bermeshev, V.P. Zhereb, M.P. Bundin, A.S. Yasinsky, O.V. Yushkova, D.S. Voroshilov, A.S. Samoilo, E.V. Mazurova, A.N. Zaloga, O.V. Yakivyuk, P.O. Yur'ev, "Effect of heat treatment of molten $6Bi_2O_3 \cdot SiO_2$ on the phase composition and microstructure of its solidification products", *Inorg. Mater*., **58** [11] (2022) 1168–1178.

16. L.T. Denisova, L.A. Irtyugo, V.M. Denisov, "Heat capacity of oxides in the Bi_2O_3-SiO_2 system", *Phys. Solid State*, **56** (2014) 2146–2148.
17. M. Back, E. Casagrande, E. Trave, D. Cristofori, E. Ambrosi, F. Dallo, M. Roman, J. Ueda, J. Xu, S. Tanabe, A. Benedetti, P. Riello, "Confined-melting-assisted synthesis of bismuth silicate glass-ceramic nanoparticles: formation and optical thermometry investigation", *ACS Appl. Mater. Interfaces*, **12** (2020) 55195–55204.
18. V.P. Zhereb, T.V. Bermeshev, Y.F. Kargin, E.V. Mazurova, V.M. Denisov, "Phase composition and microstructure of crystallization products of molten $Bi_2O_3 \cdot GeO_2$ under various cooling conditions", *Inorg. Mater*., **55** [7] (2019) 737–747.
19. A.V. Shabalina, A.G. Golubovskaya, E.D. Fakhrutdinova, S.A. Kulinich, O.V. Vodyankina, V.A. Svetlichyi, "Phase and structural thermal evolution of Bi–Si–O catalysts obtained via laser ablation", *Nanomaterials*, **12** (2022) 4101.
20. V. Vlasenko, M. Nowagiel, M. Wasiucionek, T.K. Pietrzak, "Stabilization of δ-like Bi_2O_3 Phase at Room Temperature in Binary and Ternary Bismuthate Glass Systems with Al_2O_3, SiO_2, GeO_2, and B_2O_3", *Materials*, **17** [16] (2024) 4023.
21. Z.G. Zhang, X.F. Wang, Q.Q. Tian, "Grain orientation distribution and development of grain line in highly ordered $Bi_4Si_3O_{12}$ micro-crystals", *Sci. Sintering*, 42 (2010) 51–59.
22. Z.G. Zhang, Z.Y. Jiang, X.F. Wang, Q.Q. Tian, "Correlation between grain deviation angles and the partial ordering transformation of grain line in $Bi_4Si_3O_{12}$ microcrystals", *Sci. Sintering*, **44** (2012) 257–264.
23. A.K. Boukellal, M. Sarebanzadeh, A. Orozco-Caballero, F. Sket, J. Llorca, D. Tourret, "Grain growth competition and formation of grain boundaries during solidification of hcp alloys", *Acta Mater*., **269** (2024) 119830.
24. Y.G. Song, F.L. Mota, D. Tourret, K.H. Ji, B. Billia, R. Trivedi, N. Bergeon, A. Karma, *Nat. Commun*., **14** (2023) 2244.
25. T. Takaki, "Phase-field modeling and simulations of dendrite growth", *ISIJ Int.*, **54** (2014) 437–444.
26. M. Amoorezaei, S. Gurevich, N. Provatas, "Orientation selection in solidification patterning", *Acta Mater*., **60** (2012) 657-663.
27. L. Wang, L.S. Yang, *Eur. Phys. J. E*, **43** (2020) 48.
28. H.-B. Zeng, X.-G. Ai, M. Chen, R. Guan, Y.-F. Chao, J.-C. Zhang, "Phase-field simulation study on dendritic growth behavior during bilateral directional solidification", *Mater. Today Commun*., **40** (2024) 109618.